

Control of a Double-Fed Induction Generator for Wind-Power Plants

W. Hofmann A. Thieme

Lehrstuhl Elektrische Maschinen und Antriebe
Technische Universität Chemnitz
Reichenhainer Str. 70
D-09126 Chemnitz

Abstract

The paper refers to a realized 600 kVA wind power generator system with a speed-variable electric converter based on a double-fed induction machine. The wind power station is previewed for operation in a net-parallel mode therefore the controlled induction generator system works in a line-voltage oriented reference frame. To obtain the maximal power yield a special torque reference curve has been used for generating the reference values for torque and power-factor control-loops. The measured results are discussed with regard of the desired adjustment of power.

1. Introduction

The technic of electric wind-power conversion has been developing in a violent manner during the last decades. One reason of this is due to new opportunities of power electronics. While the direct line-connected generators has been used in smaller-sized plants, the greater of them above 500 kW require to work at higher efficiency during the conversion process /1/.

Therefore it exists a competition between synchronous and asynchronous principles. With using of synchronous generators the gearbox can be replaced by a multipole machine configuration /2/.

The asynchronous squirrel cage machine has been introduced in connection with using of two gearboxes with different ratios, but each drive train has a stiff speed-torque characteristic /3/.

The best solution for adapting on a variable wind speed consists in a Double-Fed Asynchronous Generator (DFIG) based on a slip-ring wound rotor for working in a partial speed variable mode. /4/.

First of all such inverter system based on a rotor-side converter and a line-side inverter connected by an dc-link which allowed to realize a subsynchronous mode of the generator /5/.

Further studies e.g. in /6/,/7/ could be pointed that the introduction of two controllable inverters coupled by d-voltage link lead to a large operating range in connection with the power-speed characteristic of a wind turbine. From the design of such generation system was reported in /8/,/9/.

2. Principle of double feeding

Fig. 1 shows an operating diagram of common wind power turbines which is characterized by the power gain respectively the wind speed and the characteristic of the electrical part of the converter system based on an asynchronous generator. It can be seen that it exists a wide speed-range which should be used for an efficient power conversion from the mechanical wind power to the electrical output.

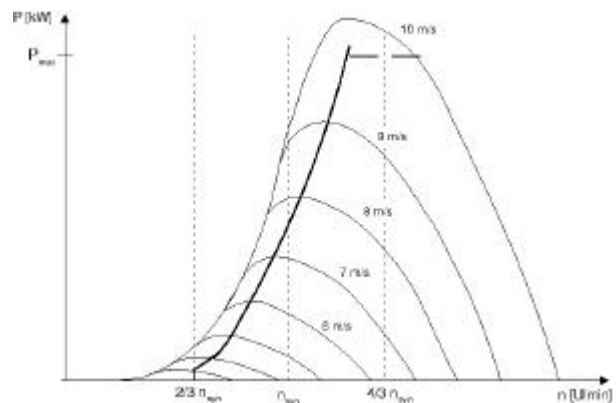


Fig. 1: Power characteristic of a wind power plant

Thereby two operating strategies can be mainly used for the power conversion :

1) Maximum power point strategy

Accordingly this operating point has to be search with the maximal power expense to exploit the given input wind energy. To reach this the power plant is working in the so-called wind-driven mode. Therefore it is necessary to use a electric converter system which make it possible to satisfy a partial speed-variable operation over a wide speed range. The advantage is the high efficiency of the total power conversion process. But it exists a certain disadvantage that the electrical power output is strongly dependent on the changes of the wind-input and we obtain a fluctuating energy flow. This principle is useable in the medium and higher wind speed regions.

2) Constant power strategy

If a pitch controlled wind-rotor is used a combined rotor-speed control and an active power regulation can be fulfilled for obtaining an approximated constant energy flow into the line-side. But it is disadvantageous because of

the non-optimal total efficiency .

To use the optimal efficiency points over a wide speed range it is necessary to put on a partial speed variable converter system which is known as the Double-Fed Induction Generator (DFIG) given in fig.2.

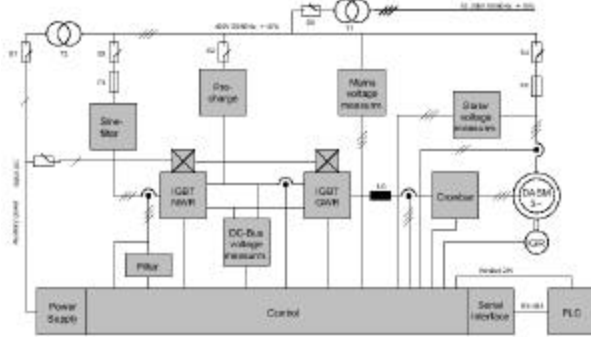


Fig.2: Double-fed induction generator system

With help of the rotor converter the slip of the induction generator can be varied and therefore the speed is changed in a wide range as shown in fig.3. If the induction generator is working with short-circuited slip-rings it works on the natural speed-torque characteristic. With more increasing of the wind-input the stability limit could be passed therefore with a energy recovery of the rotor-side the slip can be also increased and the oversynchronous mode appears. On the other hand if the wind-input decreases it is required to feed additional electric power over the slip-rings into the rotor for preventing the transition in the motor-driven mode and than the generator works in the subsynchronous mode. Because the operating range is situated optimally between $0.7 n_n < n < 1.3 n_n$ a partial speed-variable regime can be obtained. This principle is advisable because of the installed converter power rate can be reduced up to 30% of the rated values.

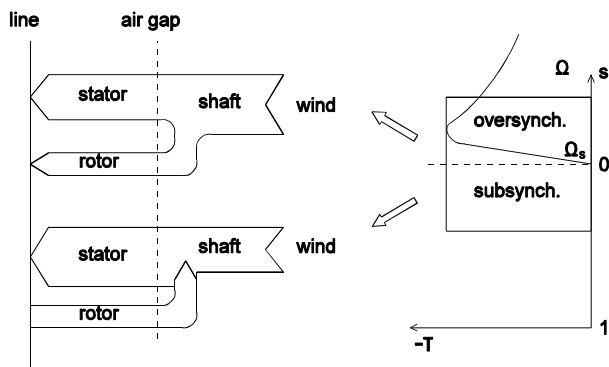


Fig.3: Operating range of the DFIG

For increasing the power rate a speed-variable and pitch-controlled system has some advantages:

- active power fluctuation can be reduced
- mechanical load steps and oscillations can be damped

- power factor can be adjusted
 - optimal power points are useable
 - line-parallel and stand-alone solutions are possible
- This paper presents the power circuits and the control configuration of a 600 kW- wind power station and gives an overview to the experimental results.

3. Fondation of the ac-generator

State space equations

The description is going out from the voltage equations in a synchronous reference frame rotating with T_k . For a better formulation it is advisable to give the state equations with variables per-unit of the ratings $U_n, I_n, S_n = 2Bf_n$. Therefore the parameters R and L become $r = R I_n / U_n$ and $x = L S_n I_n / U_n$:

$$\underline{u}_s' = r_s \underline{i}_s + \frac{d\underline{R}_s}{dt} + j T_n f_s \underline{R}_s \quad (1)$$

$$\underline{u}_r' = r_r \underline{i}_r + \frac{d\underline{R}_r}{dt} + j T_n f_r \underline{R}_r \quad (2)$$

The flux equations are independent on the reference frame with:

$$\underline{R}_s' = x_s \underline{i}_s + x_m \underline{i}_r \quad (3)$$

$$\underline{R}_r' = x_m \underline{i}_s + x_r \underline{i}_r \quad (4)$$

The electric torque is obtained with:

$$J' = \text{Im} \{ \underline{i}_s \underline{R}_s^c \} + k_r \text{Im} \{ \underline{i}_r \underline{R}_s^c \} \quad (5)$$

where $k_r = x_m / x_r$. The double fed induction generator requires the rotor voltage as control variables while the stator-voltage or line-voltage and the line-frequency f_N are constant. The rotor current phasor and the stator flux are the states variables and they can be described with:

$$\dot{\underline{R}}_r' = \left(\frac{1}{T_F} + j T_r \right) \underline{i}_r + \frac{k_s k_r}{F} \left(\frac{1}{T_s} + j T_m \right) \underline{R}_s + \frac{T_n}{F x_r} (\underline{u}_r + k_s \underline{u}_s) \quad (6)$$

$$\dot{\underline{R}}_s' = \left(\frac{1}{T_s} + j T_s \right) \underline{R}_s + \frac{x_m}{T_s} \underline{i}_r + T_n \underline{u}_s \quad (7)$$

with $T_F = F L_r / (R_r + k_s^2 R_s)$ $k_s = x_m / x_s$

$$F = 1 + x_m^2 / (x_s x_r) \quad k_r = x_m / x_r$$

The complex signal-flow diagram is shown in fig.4. and

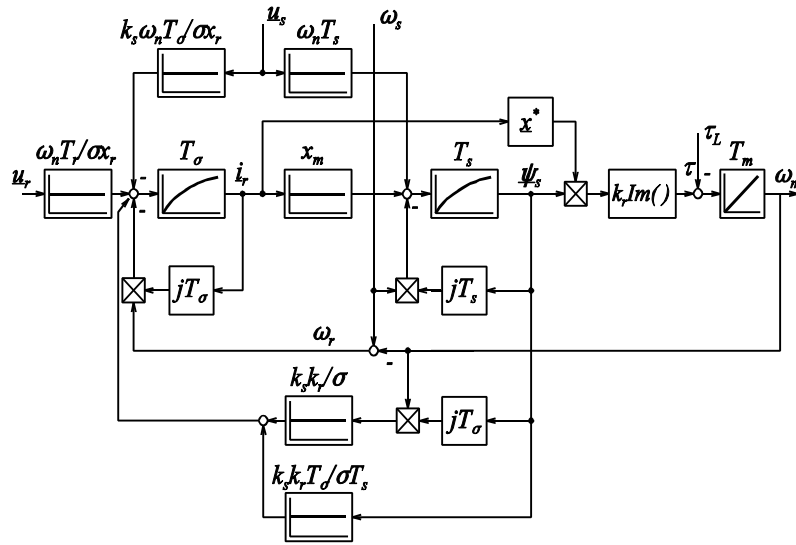


Fig.4: Complex signal flow diagram of the DFIG

describes a nonlinear coupled system which consists various phase shifting elements in form of the time-delay blocks and the imaginary operators for influences between the two orthogonal components of the rotor- current and the stator-flux phasors.

Line-voltage orientation

A common method for simplification of the nonlinear decouplings is given with the stator-flux orientation: Because of $R_{sq} = 0$ we would obtain the stator-flux with:

$$\dot{R}_{sd} \approx \frac{1}{T_s} R_{sd} + \frac{x_m}{T_s} i_{rd} + T_n u_{sd} \quad (8)$$

and from the other components the stator-frequency

$$T_s \approx \frac{x_m / T_s + j i_{rq}}{R_{sd}} + T_n u_{sq} \quad (9)$$

is determined. Before synchronizing between the DFIG and the line-voltage the stator and line-frequencies are different and is described as:

$$\theta = T_s \omega_s - T_n \omega_N \quad (10)$$

If the stator works on an isolated system or we have a unsynchronous mode between the line and the generator this so-called load-angle can be used to transform in each reference frame of the generator or the line.

If a line-parallel mode is arrived some practical advantages can be seen if the rotating reference frame is synchronized with the line-voltage. Now the stator-voltage phasor is:

$$\underline{u}_s = u_{sd} + j u_{sq} = u_s \angle \theta \quad (11)$$

and the stator-flux is approximately given with:

$$\underline{\psi}_s \approx \frac{R_{sd}}{j\omega_s} + j u_{sq} / T_s \quad (12)$$

Before feeding the electric power in the line the DFIG has to be synchronized with the stator- voltage phasor by a special PLL-controller to the line-voltage. Some kind of synchronization is shown in fig.5 .

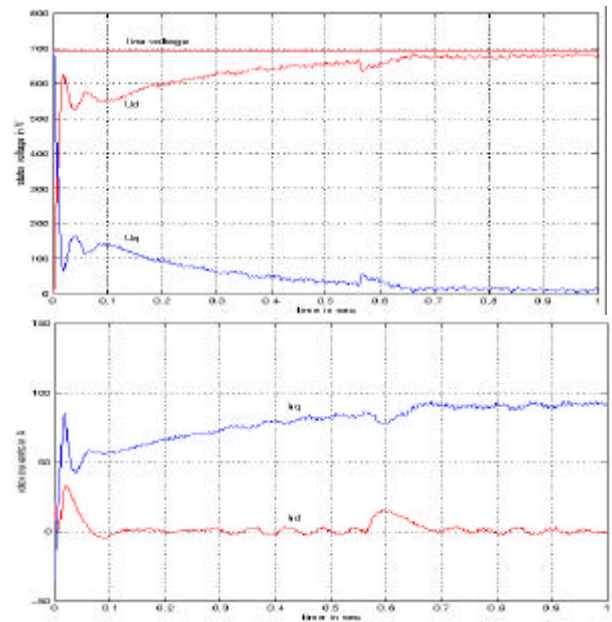


Fig.5: Synchronization in line-oriented reference frame

Both rotor-current components are used for controlling the synchronization. From equ.(6) the magnetizing can be described with:

$$\dot{R}_{sq} = \frac{1}{T_s} R_{sq} + \frac{x_m}{T_s} i_{rq} \quad (13)$$

We can see that the q-component of the rotor current determines the magnetizing state of the DFIG and the d-component control the angle of the stator voltage phasor. This is the occasion to classify the different dependencies between the control and output variables of such generator what will be further investigated in the next chapter.

4. Control schemes

Control of the generator-side inverter

The natural main control variable of such generator system should be the active power given with:

$$p_s = \text{Re} \{ \underline{u}_s \dot{i}_s^* \} = u_s i_{sd} + u_s i_{rd} \quad (14)$$

because the summarized current of the stator and rotor is a poor inductive current for magnetizing as shown in fig.6 with the phasor diagram at a constant power factor. Because the wind power station works in a line-parallel mode the active power corresponds with the electromagnetic torque:

$$J = k_s \text{Im} \{ \underline{R}_s \dot{i}_r^* \} = u_s i_{rd} / T_s \quad (15)$$

This equivalent control variable can be used besides to damp mechanical oscillations in the drive train.

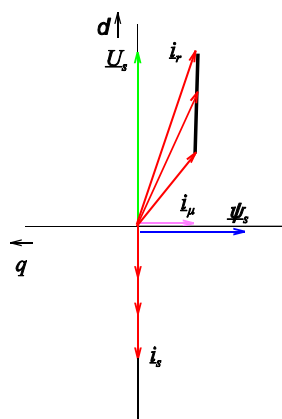


Fig.6: Phasor diagram of the active power control

In addition to the active power the converter system produces reactive power given with:

$$q_s = \text{Im} \{ \underline{u}_s \dot{i}_s^* \} = u_s i_{sq} = u_s (u_s/x_m + i_{rq}) \quad (16)$$

Fig.7 shows the phasor diagram at constant active power. Because the power factor gives a better relation as the absolute value of the reactive component the corresponding angle is introduced as control variable with:

$$(\sin) \mu = i_{sq} / i_s^* \quad (17)$$

This value is changed with help of the q-component of the rotor current.

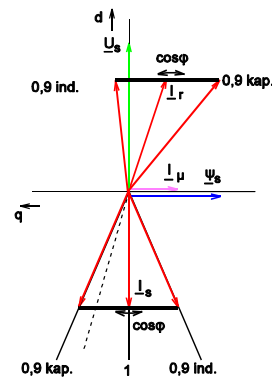


Fig.7: Phasor diagram of power factor control

After that the transfer functions for both controlled variables show the autonomous reaction of the electromagnetic torque after changing of the direct rotor current component. The quadrature rotor current component built the stator flux and influences the power factor. There are couplings between both components over the rotor current amplitude as shown in fig.8.

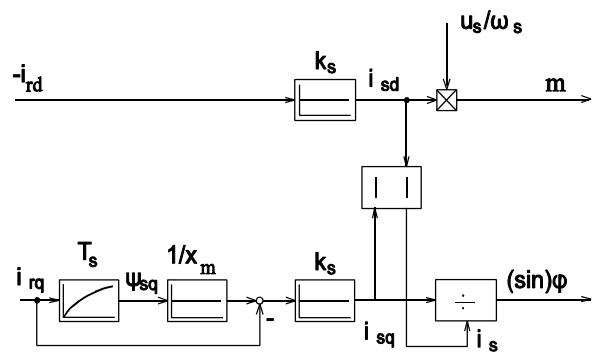


Fig.8: Bloc diagram of the rotor control system

Control of the line-side inverter

The fundamental connection between the line-voltage and the controlled inverter output-voltage u_c can be described in analogy to a synchronous generator with the phasor

diagram of fig.9 and shows as follows:

With help of the reference value of the direct component of the line-converter current i_{Nd} the size and the direction of the active power flow can be given. The positive component is connected with the subsynchronous mode and respectively the negative with the oversynchronous. If we change the quadrature component of the converter input current i_{Nq} the reactive power can be influenced and we obtain a capacitive behavior with positive and an inductive mode with negative components.

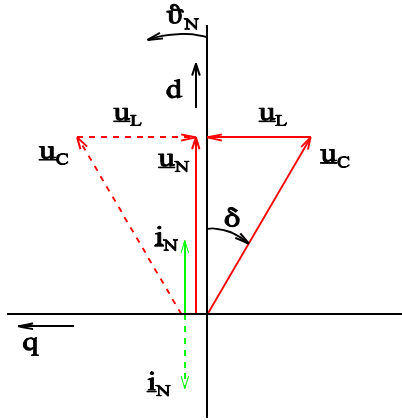


Fig.9: Line-converter diagram

The line-sided variables are defined with help of the orientation of the line-voltage. Therefore the inverter output voltage is:

$$\underline{u}_c = \ddot{u} e^{j(h_N \delta^*)} u_d, \quad (* = \hat{E}(\underline{u}_N, \underline{u}_c)) \quad (18)$$

what means that the inverter has a complex transfer function. The line-sided current results from both voltages with with neglecting the sinus-filter transfer function:

$$\underline{i}_N = \frac{1}{T_N} (\underline{u}_N \& \underline{u}_c) = \frac{1}{T_N} (u_N \& u_c e^{j^*}) \quad (19)$$

From the power resumee the dc-link current can be obtained:

$$i_{d1} = \frac{1}{u_d} \text{Re}\{\underline{u}_c \underline{i}_N^c\} = \ddot{u} (i_{Nd} \cos^* i_{Nq} \sin^*) \quad (20)$$

It follows the bloc diagram in fig. 10. The couplings are more difficult as on the rotor-side, but for small signal changes we can neglect these influences.

The dc-link voltage can be controlled by the direct line-converter sided current while the other component is responsible for the power- angle.

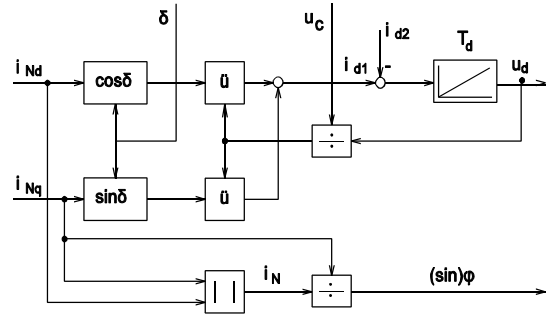


Fig.10: Bloc diagram of the net-side inverter

Control of the wind power plant

The total control structure is from a high complexity. We can decide it in a plant-side and in an converter-side part as shown in fig.11.

The process-side part is implemented in a SPC-controller where as well the mode control, the azimuth detection and its control, the modem monitoring, the fault listing, as the pitch control and the torque-optimization for references passing is realized.

The electric-side part is implemented in two micro-controllers of SIEMENS-type 80C167 assigned to each inverter. The references of the power-angle and of the electromagnetic torque is passing from the SPS.

The torque controller is optimized as an loop for reference changes. The power-angle control is determined by a division of the line-side phase-angle for control of each inverter resulting from a reactive power outcome.

The optimization is realized for a slower step response after a reference change. Than we have also a dc-link voltage controller which is adjusted of disturbance-optimal control.

Assigned to each inverter two fast current controllers are underlayed. They are equipped with the usual decoupling networks between both current components. The controllers on the rotor-side work with a PI-algorithm and those of the line-side with a dead-beat behavior designed for two steps.

The line-side converter has to be synchronized with the line-voltage. This function is taken on by a Phase-Look-loop which is synchronized of one line-phase. A slow integral controller guaranties a moderate change of the line-voltage angle which is used to coordinate the transformation of the diverse controlled variables into the line-oriented reference frame.

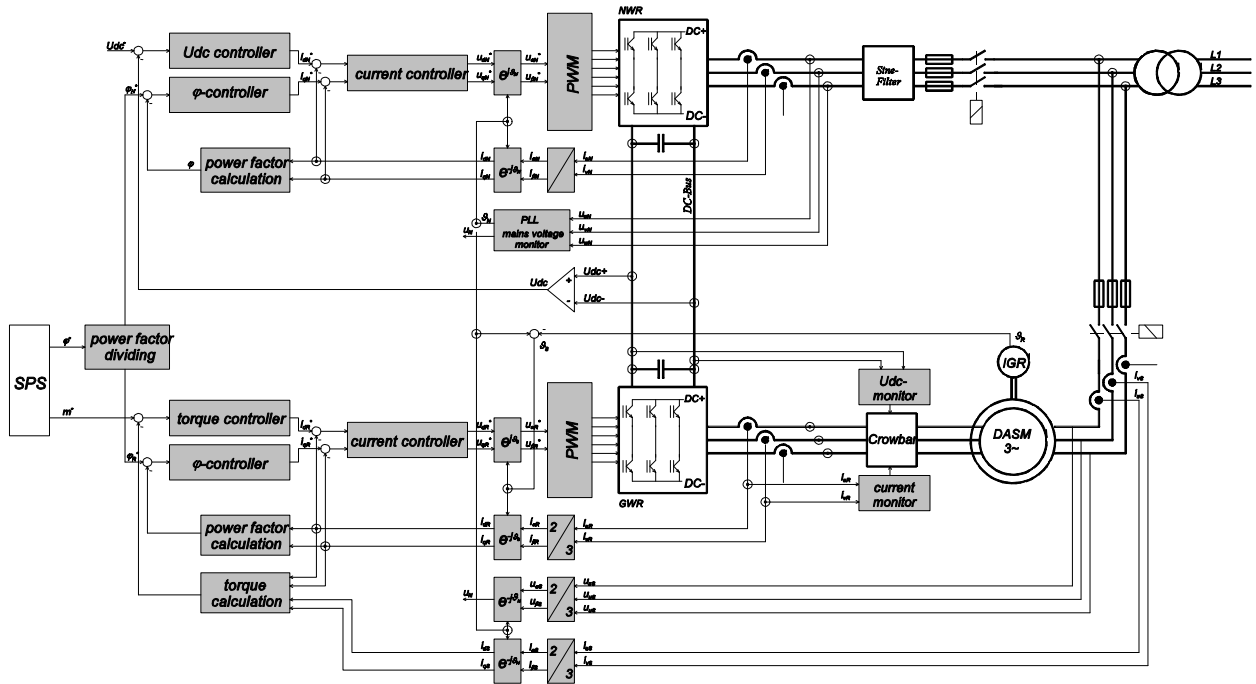


Fig.11: Control of the windpower plant

The electromagnetic torque and the power factor are calculated after coordinate transformation of the respective currents and voltages. Because as well the rotor current as the stator current can be measured it was nearly to use both controlled variables for determining the torque, but the saturation effect dependent on the size of voltage led to a modified calculation with:

$$J' \cdot x_m \operatorname{Im} \{ \dot{i}_s \dot{i}_r^c \} \cdot k_s \frac{u_s}{T_s} i_{rd} \quad (21)$$

The program flow is organized in diverse tasks with different sampling-times. The inner control-loops work in 0.5 ms and the upper loops in a 2.5 ms time-period. The state-control for the mode control is realized with a 10 ms time-sequence and the communication with a PC or SPS works in the background.

5. Performance of the electric converter

Dynamic performance

The dynamic characteristics are determined mainly by the design of the power electronics components. For the 600 kW basis variante so-called integrated power modules (IPM) with RCD snubbers have been used in the line-side and rotor-side inverters. They are configured in 3 parallel modules to 260 A r.m.s. current and 1400 V blocking voltage. These power modules allow to operate the inverters with a switching frequency of 2 kHz.

Therefore the inner control-loops can react in a very fast time-period. In the 1.5 MW plant we can find a further parallel connecting of such 3 phase power elements, but the switching frequency must be reduced to 1 kHz because of the higher switching losses and the limited cooling capacity.

The good performance of the main control can be seen on the example of step responses after reference changes of the electric torque and the power factor. The behavior of the each other controlled variables shows the autonomous mode of the control loops, shown in fig.12 .

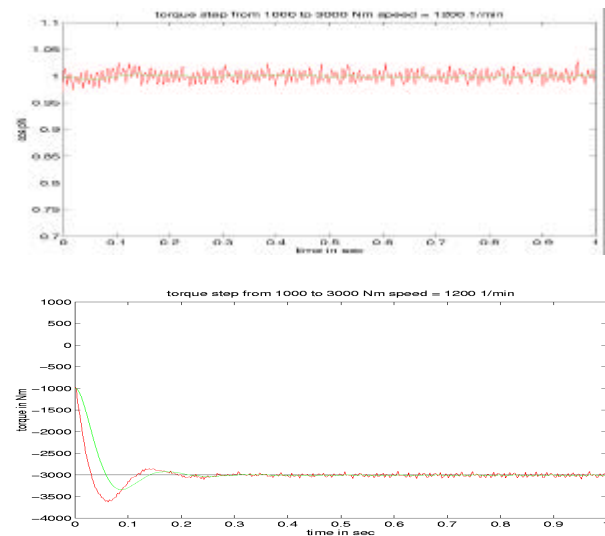
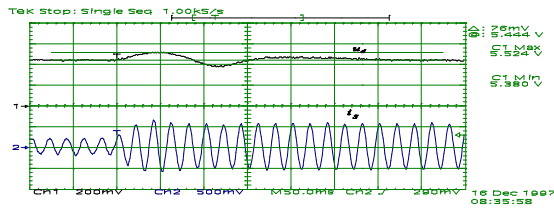
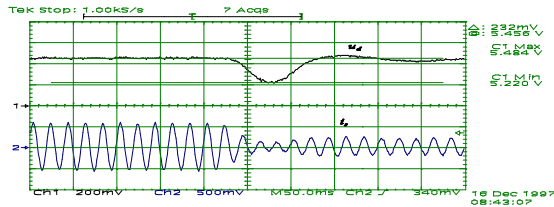


Fig.12: Step-response of torque reference step



a) loading



b) unloading

Fig.13: DC-link voltage control in oversynchronous mode

The dc-link voltage control has a main function for safe operation of both inverters and has been designed as a set-value controller. Fig. 13 shows the dynamic behavior in the oversynchronous mode. It can be seen that in the case of electric loading the energy flow from the generator air gap to the rotor increases because a certain part of the total electric energy is divided over the stator and rotor side. The voltage controller reacts with a lower direct line-converter current component and the energy of the dc-capacity can be reduced. After electric unloading in the same operation range we find the reverse reaction. The behavior in the subsynchronous range has to be reversed because the stationary energy flow over the rotor is directed from the line to the rotor.

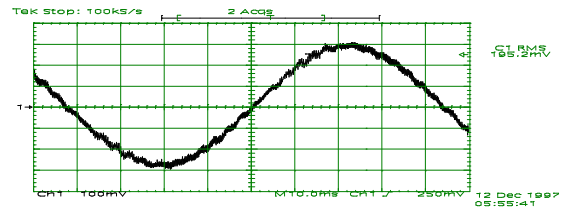
Stationary performance

The quality of the power conversion is not alone dependent on the control capability as also determined of the harmonic content. The use of an IGBT-conversion system gives us the possibility to reduce the THD-value in a wide operation range. Because the pulse-frequency is fixed on the value of 2 kHz we can observe the main harmonics in nearly band of 2 kHz. The reason is the use of the inverter control method with space-phasor modulation.

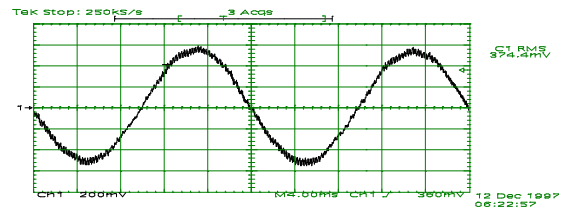
The measurement of various variables show that in the case of load and partial load the harmonic contents is very small so that the THD-value is smaller than 1%. This is valid especially for the stator current as shown in fig.14. The inverter-dependent harmonics are reduced by the generator delay-time behavior. On the other side from the line-side inverter we have higher harmonic amplitudes. These can be reduced by using of a line-filter. It consists of a star-connected ac-capacitor bank in serie with slow resistances. In fig.14 the influence of this filter in connection with the line-side inductances leads to the

improvement of the power quality. Besides this methods we have to consider that the part of the rotor-side energy contribution in the rated operation point of 600 kW is about 100 A compared with 500 A from the stator-side.

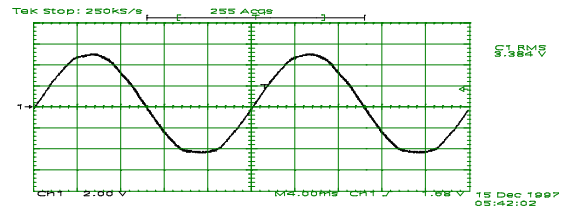
The power quality in the unload regime shows another impression because we measure a little bit higher amplitudes of the 5th and 7th harmonics. This disadvantage will be improved in the future.



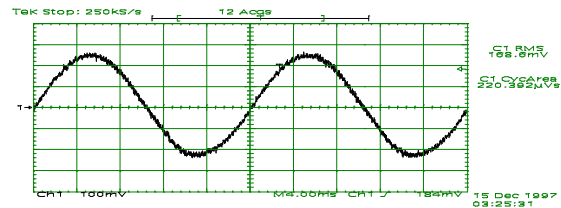
a) Rotor current 195 A r.m.s.



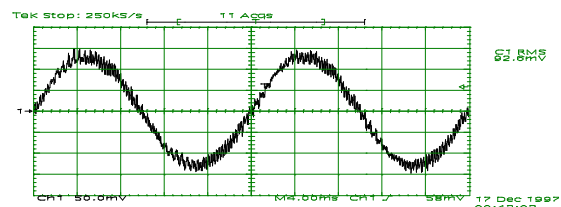
b) Stator current 375 A r.m.s.



c) Line-voltage 685 V r.m.s.



d) Line-side converter current with filtering 169 A r.m.s.



e) Line-side converter current before filtering 92 A r.m.s.

Fig.14: Stationary behaviour

6. Power quality of the windpower output

The preferred method of the windpower plant operating has been oriented on a maximum power outcome as shown in chapter 2. This requires to operate between 15 to 28 rpm of the wind rotor speed in a wind-driven mode. Corresponding to the optimal power curve a speed-dependent torque reference characteristic has been used. The torque reference is limited on the maximal torque above 28 rpm. as shown in fig.15.

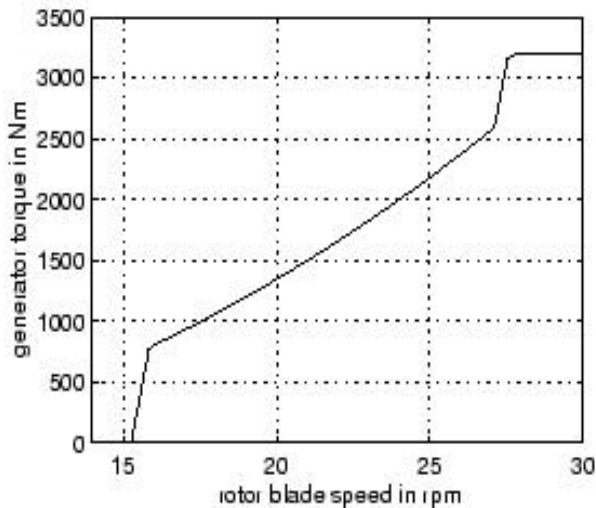


Fig.15: Torque reference curve

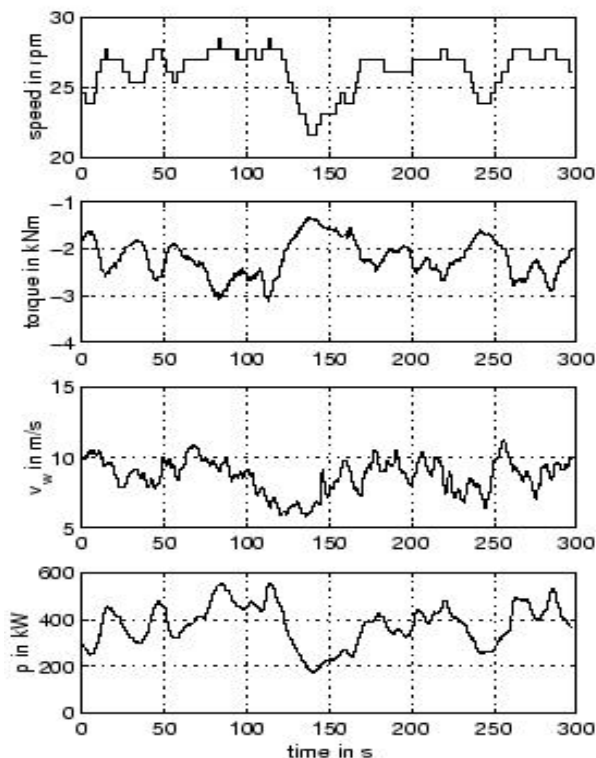


Fig.16: Measured controlled values of the plant

The strategy can be well-observed over a measured time-intervall of 300 sec, see fig.16. Because the air-velocity changes between 6 to 10 m/s the windrotor speed and the controlled electromagnetic torque are followed with a certain delay. Finally the active power reaches the maximum accordingly the working point. For minimizing the effects on the flickers the changing rate of the torque reference has been reduced by a one-second change horizon.

7. Summary

The control structure and some special methods for improving the power quality of a pitch controlled windpower station (600 kW) has been presented. The results have been shown that all mainly requirements on a modern high-power wind-driven system has been able to fulfilled.

These results are the prerequisites for adopting this principle to a 1.5 MW -plant.

The authors thank for the co-operation with the Integral Drive Systems AG (Zürich) and the WINDTEC GmbH from Austria.

8. References

- /1/ Gasch, R.: Windkraftanlagen. B.G. Teubner Stuttgart 1993
- /2/ Wobben, A.: The benchmark in Windenergy Technology. ENERCON-40. 1995
- /3/ Datenblatt Tacke: TW600 / TW600e. Tacke Windenergie GmbH 1996
- /4/ Albrecht, P.: Die geregelte doppeltgespeiste Asynchronmaschine als drehzahlvariabler Generator am Netz. Dissertation TU Braunschweig. 1984
- /5/ Warnke, O.: Einsatz der doppeltgespeisten Asynchronmaschine in einer grossen Windenergieanlage. Siemens Energietechnik 5, 1983. H. 6 Seite 362-367
- /6/ Cadirici, I.; Ermis, M.: Double-output induction generator operating at subsynchronous and supersynchronous speeds: steady-state performance optimisation and wind-energy recovery. IEE Proceedings-B Vol. 139, No.5. (1992) pp 429-441
- /7/ Pena, R.; Clare, J.C., Asher, G.M.: Doubly fed induction generator using back to back PWM converters and its application to variable-speed wind-energy generation. IEE-Proc. Electr. Power Appl. 1996, No.3. pp.231-240
- /8/ Hofmann, W.; Thieme, A.; Dietrich, A.; Stoev, A.: Design and Control of a Wind Power Station with Double fed Induction Generator EPE'97 Sept. 1997 pp. 2.723 - 2.728
- /9/ Quang, N.P.; Dittrich, A.; Thieme, A.: Doubly-fed induction machine as generator: control algorithms with decoupling of torque and power factor. Electrical Engineering 80 (1997) p.325-335